CONTENTS

ABSTRACT

High-strength ferrous and titanium alloys are of interest for use in complex structures, such as deep-diving vehicles and aircraft. A knowledge of the notch fracture toughness of these alloys is necessary to preclude catastrophic failure; however, experience indicates that no single test method itself can provide reliable fracture-toughness information across the whole toughness spectrum of these high-strength alloys.

A previously established relationship between the dynamic tear (DT) test (formally designated as the drop-weight tear test, DWTT) energy and the explosion tear test performance provides reliable fracture-toughness information of those alloys characterized by a toughness level requiring plastic deformation to propagate fracture. This analysis has not been extended to the ultrahigh-strength alloys in which fracture can propagate catastrophically at elastic stress levels. For these alloys, the analytical methods of linear elastic fracture mechanics provide the required elastic stress level and flaw-size relationship for fracture. This report deals with a "marriage" of the two approaches—the engineering and the analytical—by correlative techniques.

A direct correlation has been found to exist between the DT test energy for fracture and the critical stress intensity factor K_{Ic} for titanium alloys and steels. The relationship may also be expressed in terms of β_{Ic} — DT test energy or G_{Ic} — DT test energy. A correspondence was further established between β_{Ic} and fracture appearance as determined by the percentage of shear lip on the single-edge notch specimen. The Charpy V-notch test proved to be relatively insensitive to changes in fracture toughness of titanium alloys, and the results could not be correlated with K_{Ic}; however, such a relationship was established between these tests for steels.

The implication of this study is that reasonable estimates of plane-strain fracture toughness should be possible from results obtained from reliable engineering methods for measuring fracture toughness.

PROBLEM STATUS

This is an interim report; work is continuing.

AUTHORIZATION

NRL Problem F01-17
Project S-4607-11894

Manuscript submitted April 29, 1968.

CORRELATION OF TWO FRACTURE TOUGHNESS TESTS FOR TITANIUM AND FERROUS ALLOYS

INTRODUCTION

The Navy has a special interest in the investigation of metallurgical properties of high-strength metals to ensure the failure-safe use of these materials in large, complex structures. It is particularly important to the designer that the material selected for an application possess sufficient toughness to prevent the occurrence of catastrophic failure under elastic stress levels. Among the methods used to determine fracture toughness are the Charpy V-notch(C_v) test, the dynamic tear (DT) test (formally designated as the drop-weight tear test, (DWTT)), and tests based on linear elastic fracture mechanics.

A difficulty common to both titanium and high-strength steels in the application of the C_v test to characterize fracture toughness is the gradual change in fracture toughness over a very broad temperature range (1). This difficulty precludes the use of the transition-temperature approach in assessing the fracture-toughness characteristics of these materials, since this approach depends on an abrupt change in fracture toughness over a narrow temperature range. Furthermore, the low level of energy absorption which can be developed at temperatures corresponding to fully ductile fracture mode does not permit the assumption that a crack will arrest at a temperature associated with full shear fracture.

The DT test provides a sensitive and quantitative measure of the energy required to propagate a moving crack through the test specimen (Fig. 1). When the specimen is loaded, the embrittled weld is fractured at a low stress level, and this crack propagates into the test metal. In alloys possessing high fracture toughness, the crack tears through the test material, dissipating a significant portion of its propagation energy; brittle materials offer far less resistance to the movement of the crack.

There are two major characteristics of the DT test. The test permits full-thickness plate specimens to be used and, thereby, integrates any variation in toughness from the center to the surface of the plate. Secondly, the energy to fracture the embrittled weld and, thus, initiate a crack is usually a very small portion of the total fracture energy. This permits the separate measurement of the energy required to propagate the crack through the specimen; it is impossible in the C_v test to differentiate between initiation and propagation energy. (Highly brittle alloys may fracture under such low stress that the energy to break the weld may be a significant portion of the total DT test energy. Only an estimate of the propagation energy is possible in these cases.)

The DT test has been correlated with the explosion tear test (ETT), a structural prototype test (2). The significance of the relationship between these tests is that when crack propagation is accompanied by gross plastic deformation, the correlation permits reasonable estimates to be made from the DT test of the amount of plastic strain required to cause fracture. This correlation has not been extended to the region of elastic failure where a crack propagates at stresses below the yield point. However, it is precisely this region in which plane-strain fracture mechanics is applicable.

The rate at which elastic strain energy is released upon crack extension from a sharp flaw or fatigue crack can be determined by using fracture-toughness procedures based on linear elastic fracture mechanics. This approach assumes that the stress

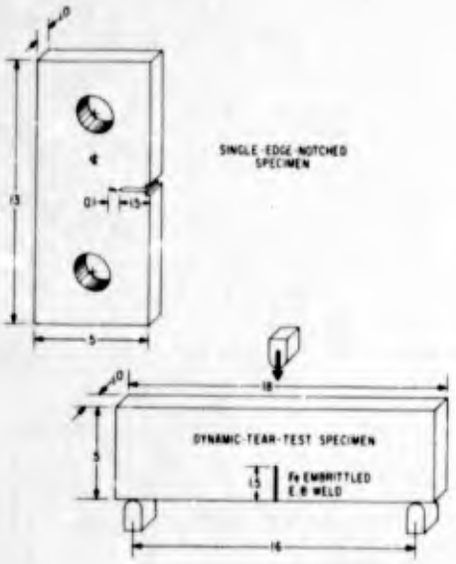

Fig. 1 - Dimensions of the single-edge-notched tension specimen (SEN) used to determine K_{Ic} values of titanium and steel alloys and the DT test specimen for titanium alloys. All dimensions are in inches.

state along most of the crack front is one of plane strain; i.e., the strain through the thickness direction of the plate is zero. One fracture-toughness parameter that may be calculated is the critical stress intensity factor for plane strain K_{Ic}, which is considered a property of the material. This parameter is a function of the nominal stress close to the crack tip and of the crack length; thus, if any two of these values are known, the third may be calculated.

The purpose of this report is to present preliminary correlations that have been developed between DT energy values and K_{Ic} for the determination of the fracture toughness of steel and titanium alloys. Further refinement of these correlations should eventually lead to the specification of reasonably accurate quantitative estimates of fracture-mechanics parameters from DT test energy measurements. In this manner, the DT values may then be expressed in terms of approximate flaw size and stress level at which initial crack extension will occur for alloys that fracture under elastic loads.

MATERIALS AND PROCEDURE

Titanium Alloys

The mechanical properties of the titanium alloys which were used in this investigation are given in Table 1. (Tension test data were obtained at room temperature.) The plates were received in the mill-annealed condition and included both standard commercial (0.15 wt-% oxygen, minimum) and very low interstitial (0.08 wt-% oxygen) grades of titanium alloys.

The fracture mechanics data for titanium alloys were obtained using both the single-edge-notched (SEN) tension specimen and the four-point-loaded notch bend (NB) specimen. All of the specimens tested were approximately 1 in. thick (except T-23), and each specimen was fatigued at a low stress to cause a crack to grow approximately 0.10 in. at the tip of the notch. The fracture-mechanics tests were conducted at room temperature.

The SEN tension specimen (Fig. 1) was modeled after that used by Sullivan (3), and the experimental compliance calibration of Ref. 3 was applied to calculate K_{Ic}. Although the calibration is independent of absolute specimen dimensions, care was taken to keep the ratio of the distance between loading-pin centers to the specimen width similar to

Table 1
Mechanical Properties of Titanium Alloys

Alloy Designation and Nominal Composition	Heat Treatment		Fracture Direction	Tension Test Data			Elongation in 2 in. (%)	Charpy-V		Dynamic Tear Test at 32°F (ft-lb)
	Solution Anneal	Aging		0.2% YS (ksi)	UTS (ksi)	R.A. (%)		32°F (ft-lb)	-80°F (ft-lb)	
T-20 Ti-6Al-4Sn-1V	As received	As received	RW	127.3	128.9	39.5	14.2	21	15	735
T-21 Ti-6Al-6V-2.5Sn	As received	As received	WR	152.0	154.5	41.5	9.5	-	-	275
T-21A Ti-6Al-6V-2.5Sn	1625°F/ 1 hr/WQ	1200°F/ 2 hr/AC	RW	166.7	170.5	22.8	10.5	13	12	421
T-21B Ti-6Al-6V-2.5Sn	1550°F/ 1 hr/AC	1200°F/ 2 hr/WQ	RW WR	129.7 135.6	139.0 142.5	31.7 27.2	15.2 15.0	17 -	15 -	550 743
T-21C Ti-6Al-6V-2.5Sn	1550°F/ 1 hr/AC	1100°F/ 2 hr/WQ	RW WR	137.2 137.2	143.4 142.0	27.6 33.6	14.5 15.2	18 19	15 15	500 717
T-21D Ti-6Al-6V-2.5Sn	1550°F/ 1 hr/WQ	900°F/ 4 hr/AC	RW	186.0	201.6	18.3	7.1	10	9	185
T-23 Ti-8Al-2Cb-1Ta	As received	As received	RW	112.0	122.2	21.0	8.0	31	28	1750*
T-27A Ti-6Al-4V	1700°F/ 1 hr/WQ	900°F/ 2 hr/AC	RW WR	132.5 140.1	150.5 155.9	25.2 23.1	10.6 10.0	20 25	18 25	1251 930
T-36 Ti-6.5Al-5Zr-1V	As received	As received	WR	124.5	131.1	21.5	12.1	20	15	960
T-55A Ti-6Al-4Zr-2Mo	1750°F/ 1 hr/WQ	1100°F/ 2 hr/AC	WR	135.7	150.6	11.2	13.2	17	17	990
T-55B Ti-6Al-4Zr-2Mo	1800°F/ 1 hr/WQ	1000°F/ 2 hr/AC	WR	132.0	147.1	13.1	9.0	23	19	748
T-67 Ti-6Al-4V-2Sn	As received	As received	RW	115.8	123.5	27.6	12.6	23	20	888
T-67A Ti-6Al-4V-2Sn	1775°F/ 1 hr/WQ	1000°F/ 2 hr/AC	RW	129.8	141.2	12.9	8.0	24	22	540
T-67B Ti-6Al-4V-2Sn	1675°F/ 1 hr/WQ	Not Aged	RW	122.0	141.6	19.1	10.5	20	16	900
T-68A Ti-6Al-4Zr-2Sn-0.5Mo-0.5V	1800°F/ 1 hr/WQ	1100°F/ 2 hr/AC	RW	117.5	130.6	18.2	11.2	18	17	1385
T-68B Ti-6Al-4Zr-2Sn-0.5Mo-0.5V	1750°F/ 1 hr/WQ	1100°F/ 2 hr/AC	RW	119.2	130.2	22.4	9.7	30	22	1470
T-68D Ti-6Al-4Zr-2Sn-0.5Mo-0.5V	1825°F/ 1 hr/WQ	900°F/ 4 hr/AC	RW	121.3	129.1	15.3	9.3	27	21	1043
T-68E Ti-6Al-4Zr-2Sn-0.5Mo-0.5V	1700°F/ 1 hr/WQ	1100°F/ 2 hr/AC	RW	121.5	138.7	14.6	9.7	24	21	1182

*This DT test value represents the WR fracture direction.

the specimen calibrated in Ref. 3. A mathematical stress analysis developed by Gross (4) provides comparable K_{Ic} values for the crack-length-to-width ratios used in these tests.

The dimensions of the NB specimen (Fig. 2) are in proportion to those recommended in Ref. 5. Pure bending was chosen over three-point loading to take advantage of the reduced influence of the shearing stress on the strain-energy release rate G. (The shearing stress is zero within the minor span.) The stress intensity factor was calculated using the boundary collocation formula for pure bending presented in Appendix A.

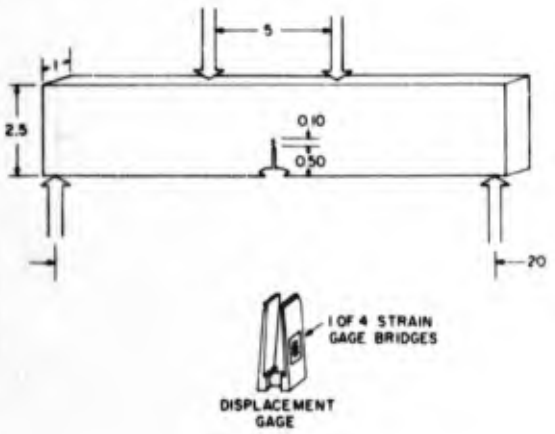

Fig. 2 - Dimensions of the four-point-loaded notch bend specimen (in inches), and a sketch of the beam displacement gage used to detect initial crack instability.

Many of the SEN and NB specimens were side-grooved to a depth of 5% of the thickness on each side of the fracture plane. Previous work has indicated that side grooves accentuate the displacement at crack instability on the load-displacement record (6). The grooves contained an included angle of 60 degrees and had a notch-root radius of 0.002 in. The method of determining K_{Ic} for side-grooved specimens is in Appendix B.

The fracture-mechanics specimens were heat treated in small batches to minimize the temperature differential among the group. A dry, flowing argon atmosphere prevented oxygen pickup during the heating cycle. All of the tensile and C_v determinations were obtained from material cut from the broken halves of these specimens.

A preliminary comparison of K_{Ic} values obtained from SEN and NB specimens is given in Table 2. The indications are that the two types of specimens will give approximately the same average K_{Ic} value.

The load-displacement graph for each K_{Ic} specimen was drawn by an X-Y recorder. When initial deviation from linearity occurred at or very near maximum load, this load value was used to calculate K_{Ic}; otherwise, the load at the lowest, distinct instability was chosen for the calculation. The detection of the initial crack extension was made with a beam displacement gage (Fig. 2), instrumented with a strain gage circuit (7). The K_{Ic} values obtained for the titanium alloys (tabulated in Table 3) are not corrected for plastic-zone size.

Table 2
A Comparison of Plane-Strain Toughness Values Obtained from SEN and NB Specimens

Alloy	Fracture Direction	K_{Ic} Values (ksi$\sqrt{in.}$)	
		SEN Specimens	NB Specimens
T-55A	WR	121 119 98	100 104 -
Average		113	102
T-55B	WR	92 95 99 102 97	92 98 - - -
Average		97	95
T-67A	RW	88 78 90 71	79 - - -
Average		82	79
T-67B	RW	96 105 106 95	112 - - -
Average		101	112

A sketch of the titanium DT test specimen is shown in Fig. 1. The DT test specimens were heat treated as 5-by-5-in. sections of 1-in.-thick plate material. Afterward, titanium tabs were electron-beam welded to the section to obtain the 18-in. specimen length. The electron-beam crack-starter welds were embrittled by diffusing Fe wire into it during the welding operation.

Steels

The ferrous alloys which were investigated include 12-Ni and 18-Ni maraging steels, 9Ni-4Co-0.25C quenched and tempered steel, 4140, D6-AC, and 5Ni-Cr-Mo-V steel. About one-half of the specimens were tested in the "as-received" mill condition, while the remainder were heat treated at NRL. The specific mill processing and NRL heat treatments are reported in Refs. 8, 9, and 10. The mechanical properties are presented in Table 4.

With one exception, all of the steel K_{Ic} data were acquired with SEN tension specimens. The experimental compliance calibration of Ref. 3 was used to compute K_{Ic}. The plane-strain plastic-zone correction was used in the computation of K_{Ic}, β_{Ic}, and G_{Ic}

Table 3
Plane-Strain Toughness Data for Titanium Alloys

Alloy Designation	Fracture Direction	Types of Specimens	Number of Specimens	K_{Ic}* Range (ksi$\sqrt{in.}$)	Average* K_{Ic} (ksi$\sqrt{in.}$)	YS (ksi)	$\left(\frac{K_{Ic}}{YS}\right)^2$ (in.)	Average Nominal Fracture Stress to Ratio $\frac{\sigma_n}{\sigma_y}$	β_{Ic}*	$\mathcal{G}_{Ic}$* (in.-lb/in.^{2})
T-20 (Ti-6Al-4Sn-1V)	RW	SEN	6	77-92	85	127.3	0.45	0.57	0.51	452
T-21 (Ti-6Al-6V-2.5Sn)	WR	SEN	2	59-63	61	152.0	0.16	0.35	0.15	233
T-21A (Ti-6Al-6V-2.5Sn)	RW	SEN	2	57-62	60	166.5	0.13	0.36	0.13	218
T-21B (Ti-6Al-6V-2.5Sn)	RW WR	SEN SEN	1 1	81 76	81 76	129.7 135.6	0.39 0.31	0.55 0.49	0.37 0.29	399 418
T-21C (Ti-6Al-6V-2.5Sn)	RW WR	SEN SEN	1 2	80 74	80 74	137.2 137.2	0.34 0.29	0.48 0.42	0.32 0.27	388 328
T-21D (Ti-6Al-6V-2.5Sn)	RW	SEN	2	32-35	34	186.0	0.03	0.16	0.03	70
T-23 (Ti-6Al-2Cb-1Ta)	RW	SEN†	-	-	115	112.0	1.06	-	1.06	828
T-27A (Ti-6Al-4V)	RW WR	SEN SEN	8 4	101-112 104-114	108 106	132.5 140.1	0.67 0.57	0.75 0.64	0.70 0.59	710 682
T-36 (Ti-6.5Al-5Zr-1V)	WR	SEN	3	91-100	96	124.5	0.59	0.75	0.55	578
T-55A (Ti-6Al-4Zr-2Mo)	WR	SEN NB	3 2	98-121	113	135.7	0.69	0.73	0.64	777
T-55B (Ti-6Al-4Zr-2Mo)	WR	SEN NB	4 2	92-102	97	132.0	0.53	0.62	0.49	559
T-67 (Ti-6Al-4V-2Sn)	RW	SEN	4	98-106	101	115.8	0.76	0.82	0.76	638
T-67A (Ti-6Al-4V-2Sn)	RW	SEN NB	4 1	71-90	82	129.8	0.40	0.56	0.43	408
T-67B (Ti-6Al-4V-2Sn)	RW	SEN NB	4 1	95-112	101	122.0	0.68	0.75	0.68	652
T-68A (Ti-6Al-4Zr-2Sn-0.5Mo-0.5V)	RW	SEN	4	117-124	119	117.5	1.02	0.91	1.00	859
T-68B (Ti-6Al-4Zr-2Sn-0.5Mo-0.5V)	RW	SEN	4	100-116	110	119.2	0.85	0.83	0.85	735
T-68D (Ti-6Al-4Zr-2Sn-0.5Mo-0.5V)	RW	SEN	3	124-131	126	121.3	1.08	0.94	1.09	965
T-68E (Ti-6Al-4Zr-2Sn-0.5Mo-0.5V)	RW	SEN	1	121	121	121.5	1.00	0.96	1.00	889

*Calculated without plastic-zone correction factor.
†Specimens of dimensions 1.5 by 0.25 by 3.3 in. (width by thickness by length) were tested by Dr. J. Krafft, Mechanics Division, NRL.

Table 4
Mechanical Properties of High-Strength Steels

Alloy Designation	Fracture Direction	Material Type	Tension Test Data				Charpy-V at 30°F (ft-lb)	Dynamic Tear Test Energy at 30°F (ft-lb)
			0.2%Ys (ksi)	UTS (ksi)	E'ong. in 2 in. (%)	RA (%)		
J-14	RW	9-4-0.25C	180.0	196.2	61.0	16.8	38	1844
J-14	WR	Mill heat treated straight rolled	180.3	196.4	48.0	15.0	30	1295
J-15	RW	9-4-0.25C	–	–	–	–	38	1996
J-15	WR	Mill heat treated 1 by 1 cross roll	183.2	195.0	61.0	17.0	40	2000
J-66	RW	12-Ni mill heat treated	–	–	–	–	29	–
J-66	WR	12-Ni mill heat treated	185.3	188.0	56.7	13.3	32	–
J-66	WR	12-Ni NRL heat treated	176.3	179.9	52.1	13.5	38	–
J-67	RW	12-Ni mill heat treated	178.6	182.3	57.2	15.0	34	–
J-67	WR	12-Ni mill heat treated	–	–	–	–	31	–
J-67	WR	12-Ni NRL heat treated	178.0	181.9	54.9	14.0	40	–
J-68	WR	12-Ni mill heat treated	171.2*	177.2*	49.1*	14.0*	21	744
J-68	WR	12-Ni NRL heat treated	180.7	183.5	51.9	12.0	36	1630
J-70	WR	9-4-0.25 mill heat treated	176.3	186.6	55.2	16.0	40	2112
J-70	WR	9-4-0.25 NRL heat treated	186.1	198.0	55.2	16.0	36	1280
J-71	WR	12-Ni mill heat treated	176.8	183.2	59.6	14.5	42	–
J-71	WR	12-Ni NRL heat treated	174.9	179.2	64.1	15.0	74	4340
J-72	WR	12-Ni mill heat treated	177.3	183.3	59.2	14.5	47	3251
J-72	WR	12-Ni NRL heat treated	177.1	180.2	63.4	16.0	65	3538
J-78	WR	12-Ni mill heat treated	185.5	188.7	59.7	14.0	41	2271
J-78	WR	12-Ni NRL heat treated	189.4	192.2	54.6	12.5	44	2176
J-87	WR	9-4-0.25 mill heat treated	179.2	189.4	60.5	17.0	39	1996
J-87	WR	9-4-0.25 NRL heat treated	169.7	178.5	51.4	16.5	42	2026
J-88	WR	9-4-0.25 mill heat treated	180.2	191.3	54.1	16.0	42	1692
J-88	WR	9-4-0.25 NRL heat treated	168.3	178.6	63.6	18.0	42	2186
H-57	WR	4140 NRL heat treated	176.6	194.8	32.6	9.5	14	593
D-63A	RW	18-Ni mill heat treated	229.5	240.3	9.0	45.9	24	400-500
D-63B	RW	18-Ni mill heat treated	234.5†	245.7†	7.0†	29.2†	–	400-500
D-6AC	–	NRL heat treated	212	229	12.0	44.6	20	–
I-79 (2" thick)	WR	5-Ni mill heat treated	144	150	65.0	19.0	92	–

*These values are for the EW fracture direction.
†These values represent the WR fracture direction.

(tabulated in Table 5), although the uncorrected K_{Ic} values are also reported for comparison. As with the titanium alloys, the K_{Ic} tests were conducted at room temperature.

The DT test specimen used for the high-strength steels was slightly different from that depicted in Fig. 1. The electron-beam crack-starter weld was 2 in. in length rather than the 1.5 in. indicated. Titanium wire was diffused through the thickness of the steel specimen to cause embrittlement of the electron-beam crack-starter weld.

TEST RESULTS AND DISCUSSION

Relationship Between the Critical Stress Intensity Factor K_{Ic} and Yield Strength

A plot of the titanium K_{Ic} data against yield strength (ys) at 0.2% offset is shown in Fig. 3. Each data point represents a particular alloy and heat treatment; the RW and WR fracture directions (11) are identified, respectively, by a horizontal or vertical line drawn through each point. The graph indicates that an inverse relationship exists between K_{Ic} fracture toughness and ys for titanium alloys. The ys values range from a low of 112 ksi to a high of 186 ksi for the alloy Ti-6Al-6V-2.5Sn. The number of specimens and range of K_{Ic} numbers obtained for each are recorded in Table 3.

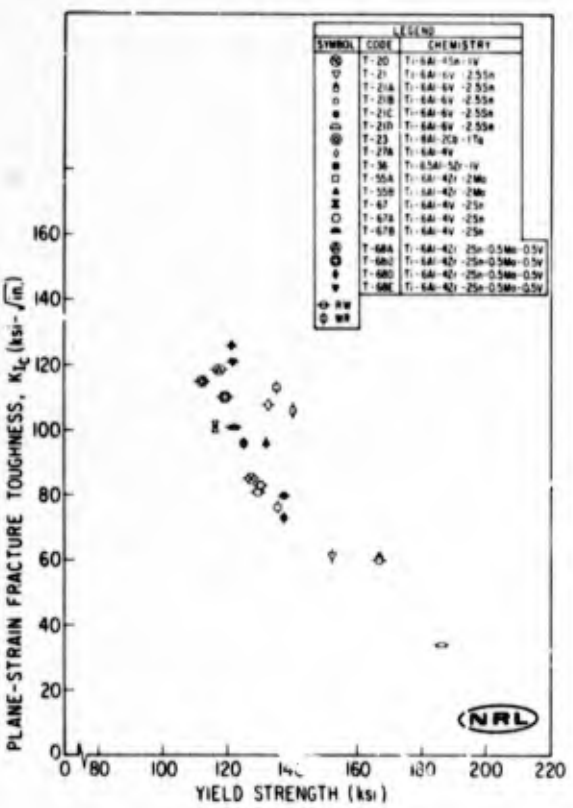

Fig. 3 - K_{Ic} versus ys for several titanium alloys heat treated to various levels of toughness

Table 5
Plane-Strain Fracture Toughness Data for High-Strength Steels

Alloy Designation	Fracture Direction	YS (ksi)	Dynamic Tear Test Energy at 30°F (ft-lb)	Number of Specimens	K_{Ic}* Range (ksi $\sqrt{in.}$)	Average* K_{Ic} (ksi $\sqrt{in.}$)	Average* β_{Ic}	Young's Modulus (ksi)	Average* $\mathcal{G}_{Ic}$ (in.-lb/in.^{2})	Average Nominal Stress to YS Ratio, σ_n/σ_y	Average† K_{Ic} (ksi $\sqrt{in.}$)
J-14	RW	180.0	1844	2	158-165	162	0.80	28.6	919	0.76	158
J-14	WR	180.3	1295	2	137-138	138	0.56	28.6	657	0.65	135
J-15	RW	—	1996	2	155-156	156	0.73	28.6	854	0.72	151
J-15	WR	183.2	2000	2	152-155	154	0.69	28.6	832	0.72	149
J-66	RW	—	—	1	166	166	0.80	27.5	1000	0.87	161
J-66	WR	185.3	—	2	116-124	120	0.40	27.5	524	0.58	118
J-66	WR	176.3	—	3	131-143	137	0.57	27.5	684	0.67	134
J-67	RW	178.6	—	1	153	153	0.71	27.5	852	0.74	148
J-67	WR	—	—	2	119-130	125	0.46	27.5	568	0.57	124
J-67	WR	178.0	—	3	131-137	135	0.55	27.5	666	0.68	132
J-68	WR	171.2	744	2	100	100	0.36	27.5	364	0.54	98
J-68	WR	180.7	1630	2	125-126	126	0.50	27.5	580	0.64	123
J-70	WR	176.3	2112	3	163-166	164	0.90	28.6	945	0.83	160
J-70	WR	186.1	1280	4	150-156	153	0.69	28.6	822	0.77	149
J-71	WR	176.8	—	3	198-206	203	1.22	27.5	1503	1.0	192
J-71	WR	174.9	4340	1	(252)	(252)	(1.93)	27.5	(2310)	1.2	(235)
J-72	WR	177.3	3251	3	201-213	208	1.33	27.5	1580	1.0	197
J-72	WR	177.1	3538	1	211	211	1.35	27.5	1620	1.0	200
J-78	WR	185.5	2271	1	155	155	0.70	27.5	873	0.72	150
J-78	WR	189.4	2176	2	184-192	188	1.00	27.5	1285	0.89	182
J-87	WR	179.2	1996	2	158-169	163	0.83	28.6	930	0.63	158
J-87	WR	169.7	2026	3	167-175	171	1.05	28.6	1020	0.94	165
J-88	WR	180.2	1692	3	159-166	163	0.82	28.6	930	0.62	158
J-88	WR	168.3	2186	3	164-176	169	1.04	28.6	1000	0.94	161
H-57	WR	176.6	593	3	89-91	90	0.26	29.5	274	0.48	88
D-63A	RW	229.5	400-500	1	70	70	0.09	27.0	176	0.34	69
D-63B	RW	234.5	400-500	2	75-79	77	0.11	27.0	215	0.37	76
D6AC	—	212‡	—	1	96	96	0.10	—	—	—	95
J-79	WR	144	—	2	252	252	1.31	29.5	2150	1.40	233

*Plastic-zone correction included in calculation.
†Calculated without plastic-zone correction factor.
‡This value represents WR fracture direction.

A similar inverse relationship between K_{Ic} and ys is shown in Fig. 4 for the steels. The broad spectrum of K_{Ic} values determined for a given steel within narrow ys range is an indication of significance of processing and heat-treating variables.

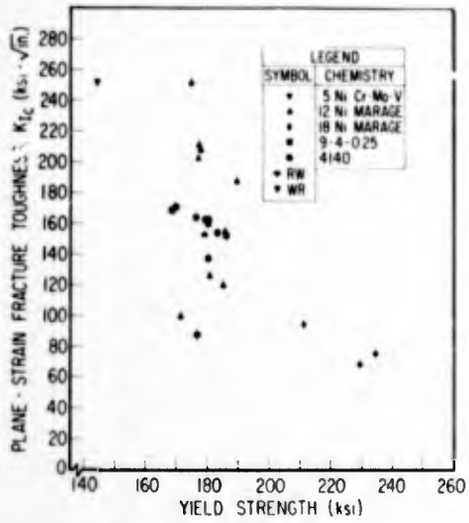

Fig. 4 - K_{Ic} versus ys for several steel alloys heat treated to various levels of toughness

Among the criteria used to determine the validity of the K_{Ic} values was the requirement that the specimen thickness equal about 2.5 times the plane-stress plastic-zone size $2r_Y$, where $2r_Y = (1/\pi)(K_I/\sigma_{ys})^2$. According to Ref. 12, the thickness B should be more than $2(2r_Y)$ for a correct K_{Ic} to be determined from a 7075-T6 aluminum alloy. The necessity of this thickness requirement was reinforced for a variety of materials in Ref. 6, which involved both smooth and side-grooved SEN specimens. The thickness needed for valid K_{Ic} appeared to be approximately $2.5(2r_Y)$, or $\beta_{Ic} \leq (1.4)$, where $\beta_{Ic} = (K_{Ic}/\sigma_{ys})^2/B$. Specimens not meeting this requirement appeared to underestimate the fracture toughness and thus fail conservatively. Currently, Committee E-24 of ASTM recommends that the thickness exceed $2.5(K_{Ic}/\sigma_{ys})^2$, or approximately $8(2r_Y)$ for a NB specimen. This requirement would preclude all data points above $\beta_{Ic} = 0.40$ in Figs. 7 and 10, if it was applied to SEN specimens. The authors believe that values significantly greater than this are representative of the plane-strain fracture toughness of a material based on the findings in Refs. 6 and 12.

Correlation of K_{Ic} and DT Test Energy

The plane-strain fracture toughness of titanium alloys is compared with DT test energy in Fig. 5. A direct correlation exists between these two fracture toughness tests; low K_{Ic} numbers are associated with low DT values.

It is evident in Fig. 5 that above about 1200 ft-lb of DT test energy, the K_{Ic} values remain essentially constant as the DT test numbers increase. This may be an indication that the stress intensity factor was underestimated for K_{Ic} values computed above 110 ksi$\sqrt{\text{in.}}$ For K_{Ic} numbers of 110 ksi$\sqrt{\text{in.}}$ and less, however, there appears to be a high degree of proportionality with DT test energy values. It may also be noted in Table 3 that the ratio of the nominal fracture stress to ys for K_{Ic} specimens approached unity for alloys which manifested K_{Ic} values approximating 120 ksi$\sqrt{\text{in.}}$ and/or DT test numbers greater than 1200 ft-lb. Thus, it is possible that the alloys within this category underwent gross yielding. Details of the nominal stress calculation appear in Appendix C.

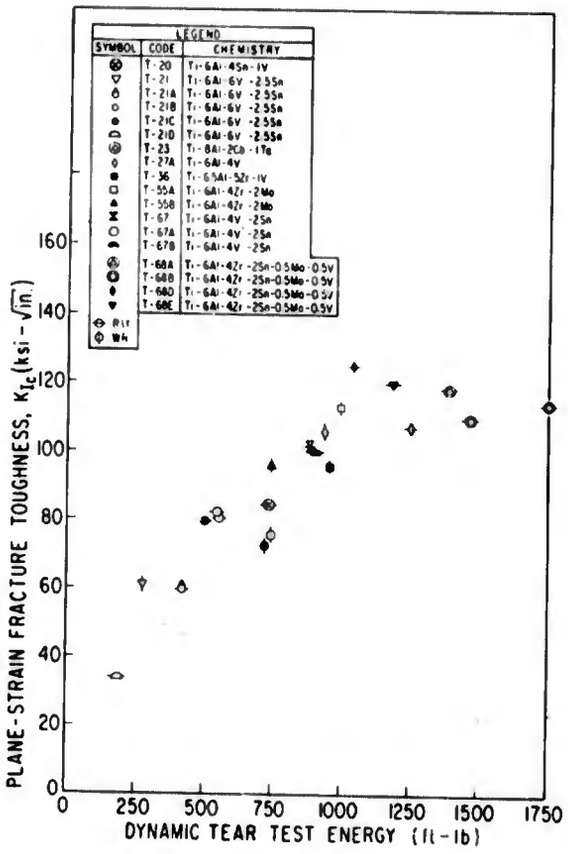

Fig. 5 - The correlation of K_{Ic} with DT Test energy for titanium alloys

The K_{Ic} values for the steels are tabulated in Table 5 and are plotted against DT test energy in Fig. 6. A direct correlation exists for K_{Ic} values of 70 to 250 ksi$\sqrt{in}$. More data will be required to determine whether the agreement is linear throughout this range of K_{Ic} values. The vertical band drawn at 3500 ft-lb on the DT test scale designates the approximate energy values at which the fracture surface of the DT test specimen becomes 100% shear (slant) fracture. The band also represents the point at which the nominal-to-ys ratio in the K_{Ic} test approaches 1.0. Beyond this value, the crack may extend by gross yielding rather than under conditions of linear elastic fracture mechanics.

Association of Shear Lip Formation with β_{Ic} and DT Test Energy for Titanium Alloys

A further insight into the fracture toughness of titanium alloys is provided in Tables 6 and 7. In Table 6 the β_{Ic} value is compared to the proportion of the SEN fracture surface which was composed of shear lips. Appendix D contains the details of this calculation. With two exceptions, T67B and T55A, there seems to be a correspondence between β_{Ic} and fracture appearance as determined by percentage of shear lip formation. The very low β_{Ic} value of T-21D is related to an essentially flat fracture surface. The β_{Ic} numbers which range between 80 and 100 ksi$\sqrt{in}$. correspond to specimens which evidence a moderate amount of shear lip (24-48%). The high β_{Ic} values generally coincide with SEN specimens in which over 70% of the broken surface is composed of shear fracture.

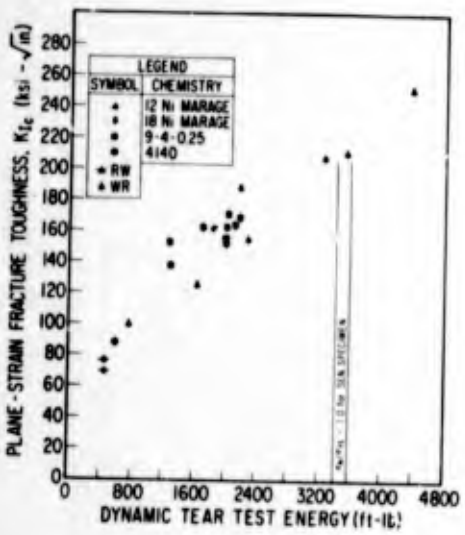

Fig. 6 - The correlation of K_{Ic} with DT test energy for steel alloys

Table 6
Relation Between β_{Ic} and the Proportion of Shear Lip Formation on the Titanium SEN Specimens

Alloy	Fracture Direction	K_{Ic} (ksi$\sqrt{in.}$)	No. of Specimens Measured	β_{Ic}	Shear Lip on SEN Specimen (%)
T-21D	RW	34	1	0.03	1
T-67A	RW	82	3	0.43	24
T-20	RW	85	2	0.51	31
T-36	WR	96	1	0.55	48
T-55B	WR	97	2	0.49	44
T-67B	RW	101	1	0.68	13
T-68B	RW	110	2	0.85	83
T-55A	WR	113	2	0.64	40
T-68A	RW	119	2	1.00	85
T-68E	RW	121	1	1.00	82
T-68D	RW	126	2	1.09	71

The relationship between the percentage of shear lip formation on the titanium DT test specimens and the DT energy values is presented in Table 7. Although this relationship contains more exceptions than did Table 6, the same general trend seems to be evident. The DT test specimens which required less than 750 ft-lb of energy to fracture generally produced little shear lip formation on the fracture surfaces. A moderate amount of shear (35-53%) was found on specimens which broke between 735 and 1000 ft-lb, whereas 75% or more was observed for specimens of more than 1000 ft-lb DT test energy.

For the area in which a high degree of correlation exists between β_{Ic} and DT test energy (less than 1200 ft-lb in Fig. 5), it might be expected that a relationship should exist between the fracture appearance of the DT test and SEN specimens. This, however,

Table 7
Comparison of DT Test Energy with the Proportion of Shear Lip Formation on Titanium Dynamic Tear Test Specimens

Alloy	Fraction Direction	Dynamic Tear Test Energy 32°F (ft-lb)	No. of Specimens Measured	Shear Lip on Dynamic Tear Test Specimen (%)
T-67A	RW	540	1	0
T-21B	RW	550	2	11
T-55B	WR	748	1	0
T-21D	RW	185	1	41
T-20	RW	735	2	35
T-67	RW	888	2	53
T-67B	RW	900	2	48
T-36	WR	960	2	46
T-55A	WR	990	1	41
T-68D	RW	1043	3	32
T-68E	RW	1182	1	75
T-68A	RW	1385	1	100
T-68B	RW	1470	1	87

does not seem to be the case. There is an indication that a high percentage of shear lip formation is associated with high β_{Ic} and DT test values, but the number of alloys on which this was evident was too small to establish a trend.

The leveling off of the K_{Ic}-DT test curve in Fig. 5 at a K_{Ic} of 110 to 120 ksi$\sqrt{\text{in.}}$ may be related to the large percentage of shear which was measured on the broken surfaces of the SEN specimens. Although there was no indication that yielding had occurred, specimens of greater thickness must be tested before it is known whether these data points represent the true plane-strain fracture toughness of the material.

Relationship of DT Test Energy with β_{Ic} and G_{Ic}

Titanium Alloys — The DT test energy is compared to β_{Ic} for titanium alloys in Fig. 7. The reason for plotting β_{Ic} was to put the stress intensity factor in a term similar to that which is used to compute the plastic-zone size. Both the resistance of the material to initial crack extension (K_{Ic} test) and its resistance to crack propagation (DT test) are a function of the plastic-zone size. The fraction $1/B$, where B is the specimen thickness, approximated unity, since the specimens were cut from 1-in. -thick plates.

The scatter of the data points increases sharply above $\beta_{Ic} = 0.75$. The reason for this sharp increase may be similar to that given for the leveling of the K_{Ic}-DT test curve of Fig. 5. The significance of Fig. 7 is that it indicates that valid K_{Ic} values may be attained with β_{Ic} as high as 0.75 for 1-in. -thick specimens. It is recognized that this contention is based on indirect evidence and that it should be verified by a program to determine if K_{Ic} remains constant for thicker specimens.

The critical-strain-energy release rate G_{Ic} is plotted against the DT test energy divided by nominal fracture area (excluding the brittle crack-starter weld of the DT test specimen) in Fig. 8. This curve was drawn to compare similar quantities on each axis (in. -lb/in.^{2}).

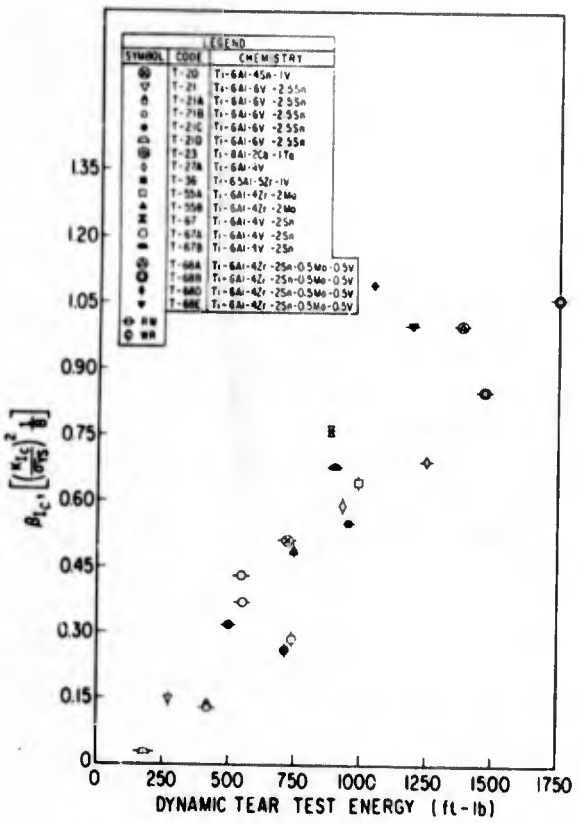

Fig. 7 - The correlation of β_{I_c} with DT test energy for titanium

The computation of $\mathcal{G}_{I_c}$ ($\mathcal{G}_{I_c} = (K_{I_c})^2/E$) involves data regarding the elastic modulus E, which is not a constant for titanium alloys but differs with both the alloy content and the heat treatment. Since the modulus was not available for all of the alloys and heat treatments used in this study, a representative value was chosen. The value depended on whether the alloy was tested in the solution-treated condition or in the solution-treated-and-aged condition. For solution-treated alloys, E equaled 16.0×10^6 psi; for solution-treated-and-aged alloys, E equaled 16.5×10^6 psi.

The $\mathcal{G}_{I_c}$-vs-DT test data show scatter similar to that of β_{I_c}-vs-DT energy data for alloys of high fracture toughness. However, below a strain-energy release rate of 700 in.-lb/in.^{2}, a particularly good correlation exists.

A correlation was attempted between the Charpy-V energy at 32°F and K_{I_c} values for titanium alloys. The excessive scatter of C_v data above K_{I_c} values of 80 ksi$\sqrt{\text{in.}}$ (Fig. 9) prevented the establishment of a meaningful relationship between these two tests. Similar problems have been previously observed in comparing C_v and DT test energy for titanium alloys (1).

Steels — The graph comparing β_{I_c} versus DT test energy for steels is presented in Fig. 10. The increase in scatter seen for the titanium alloys above $\beta_{I_c} = 0.75$ is not evident in this figure. The vertical band which intersects the abscissa at 3500 ft-lb designates the lowest approximate energy at which 100% shear fracture is present on the DT test specimen.

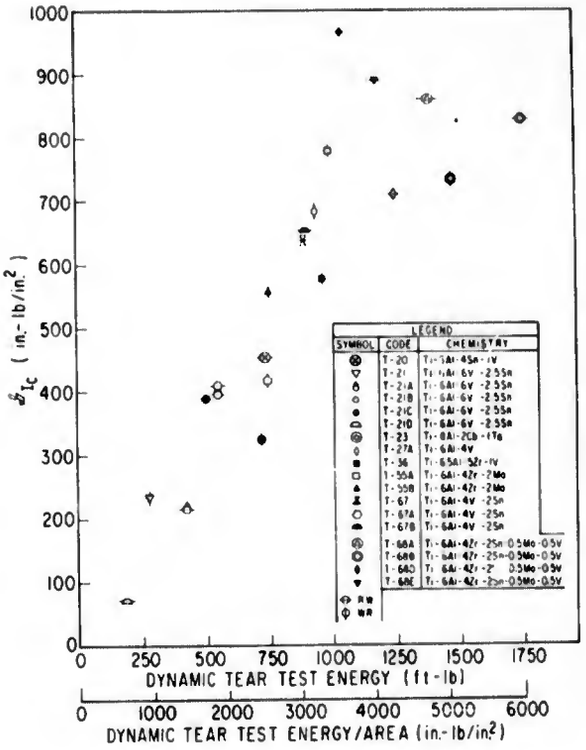

Fig. 8 - The strain-energy release rate β_{Ic} is compared to DT test energy divided by the nominal area of the fracture plane for titanium. The purpose of this graph is to provide the same units of measure on each axis.

A plot of β_{Ic} versus DT test energy divided by fracture area is shown in Fig. 11. As in the β_{Ic}-versus-DT test energy graph, the amount of scatter is minimal at this stage of development of the correlation. The values of Young's modulus E used to calculate G_{Ic} for the individual steels are tabulated in Table 5.

A plot of C_v versus K_{Ic} for high-strength steels is given in Fig. 12. The C_v values range from 14 to over 90 ft-lb. It should be noted that the C_v numbers relate to tests performed at 30°F, which corresponds to the upper shelf (maximum) energy for fracture. This is also true of the DT test energy values reported for these steels.

Factors Which May Influence the Correlations

There are several elements which might affect the accuracy of the preliminary correlations. Since K_{Ic} is influenced by the strain rate, the high rate of applied strain in the DT test may cause the specimen to fracture with a different apparent toughness than would be expected if the strain rates of the two tests were similar. Since little is known about the effect of strain rate on K_{Ic} for these alloys, the manner in which the correlations may be affected is difficult to evaluate.

An energy loss is inherent in the fracture of the DT test specimen's brittle, crack-starting weld. Although the loss is small (approximately 200 and 400 ft-lb for the titanium alloys and steels, respectively), it might be a significant portion of the energy recorded by the most brittle DT test specimens. It would be expected that this factor should cause the curves in which DT test energy is plotted to intersect the abscissa at a point offset from the origin rather than at the origin. This is demonstrated in Figs. 7, 8, 10, and 11; additional low DT test data points may be needed before it is evident in Figs. 5 and 6.

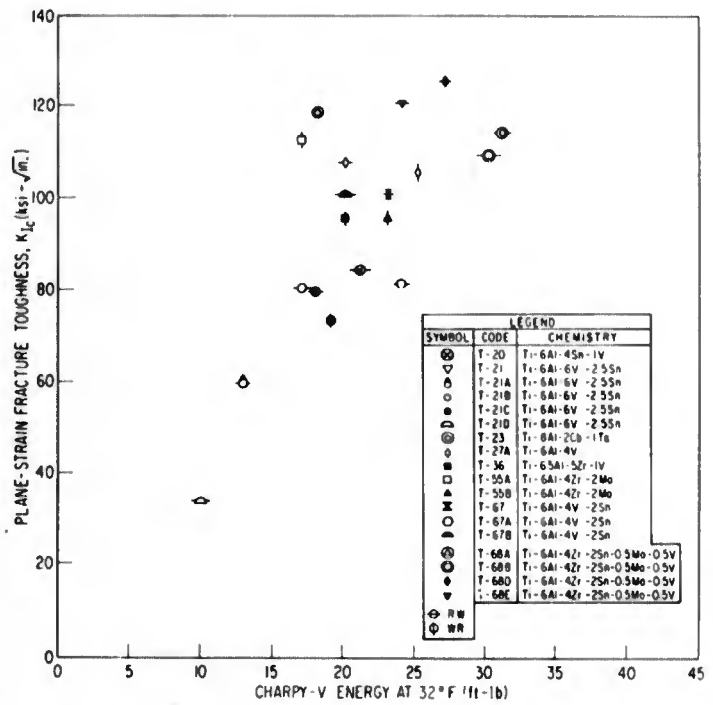

Fig. 9 - A comparison of K_{Ic} versus Charpy-V energy for titanium alloys at 32° F

A third and perhaps most important point is that as the crack tears through the DT test specimen, it may initially be governed by a plane-strain state of stress, but in the tougher alloys it will propagate primarily under a mixed-mode stress state. The mixed mode is probably caused by the lateral expansion of the crack at the same time that it moves forward. The lateral movement would effectively decrease the constraint around the crack tip and cause the stress intensity factor to rise once plane-strain conditions no longer exist. Hence, the plastic-zone size would increase in the region of mixed-mode stress state, and this would eventually produce surface relaxation manifested by shear lips. It is therefore expected that energy measured in the DT test would, for tough alloys, represent mixed mode or plane stress, whereas the stress intensity factor K_{Ic}, which is determined by local crack-tip instability, would measure plane-strain conditions. (Local crack-tip instability in tough materials involves limited crack extension; a continually rising load is required to keep the crack propagating.) Thus, the increase of the correlation scatter at higher DT test energy values might be expected.

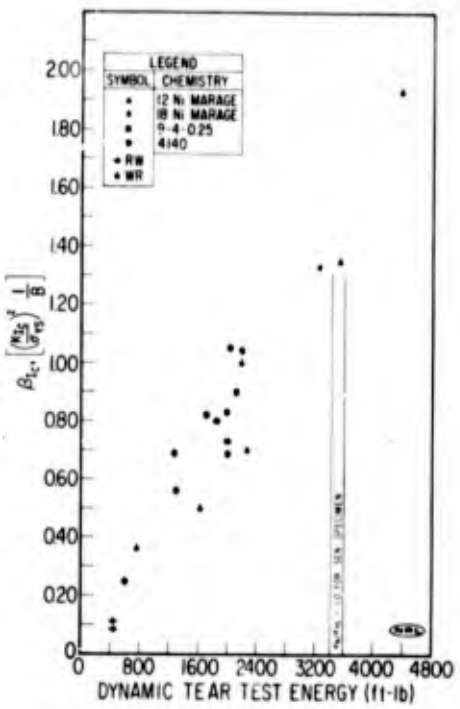

Fig. 10 - A comparison of β_{Ic} with DT test energy for steel alloys

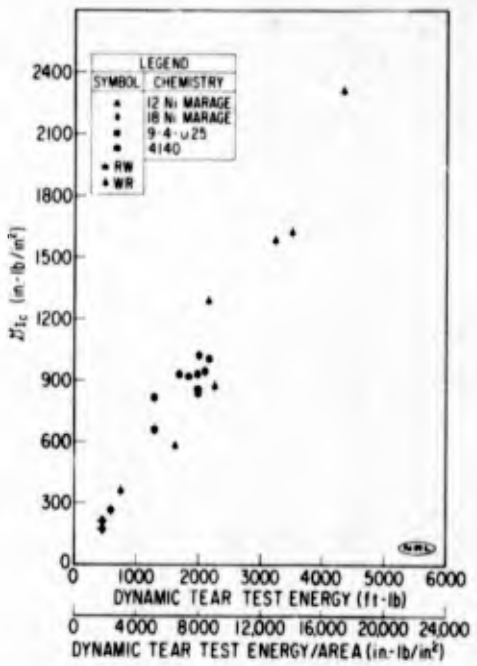

Fig. 11 - The strain energy release rate $\mathcal{G}_{Ic}$ versus DT test energy divided by the nominal area of the fracture plane for steel alloys

There is another possible explanation for the scatter of data among the titanium alloys which demonstrated high fracture toughness. No plane-strain plastic-zone correction factor was applied to the fracture-mechanics parameters determined for these alloys. Such a correction would have resulted in a small elevation of the values obtained for the high toughness materials compared to no change for the material of low toughness. This would mitigate the leveling-off of the K_{Ic}-versus-DT-test-energy curve of Fig. 5 and would lessen the scatter of Figs. 7 and 8. A plastic-zone correction was applied in the calculation of K_{Ic} for high-strength steels. Although only a few data points represent the steels of very high toughness, no significant leveling-off is observed in Fig. 6, and little scatter is noted in Figs. 10 and 11.

CONCLUSIONS

A high degree of correlation has been determined to exist between the fracture-mechanics parameters and DT test energy values for titanium alloys and steels. The relationships developed are in terms of K_{Ic} versus DT test energy, β_{Ic} versus DT test energy, and $\mathcal{G}_{Ic}$ versus DT test energy. A K_{Ic}-versus-C_v curve was also developed for steels, but excessive scatter of data above a K_{Ic} value of 80 ksi$\sqrt{\text{in.}}$ and limited data below this value precluded a correlation of these data for titanium alloys.

The usefulness of these correlations for steels and titanium alloys is twofold. They enhance the value of the low DT test energy numbers which are associated with crack propagation under elastic loading conditions in that they provide a means of using results obtained with the simpler and less expensive DT test to predict approximate values of K_{Ic}, β_{Ic}, and $\mathcal{G}_{Ic}$. With additional refinement of these correlations, more accurate

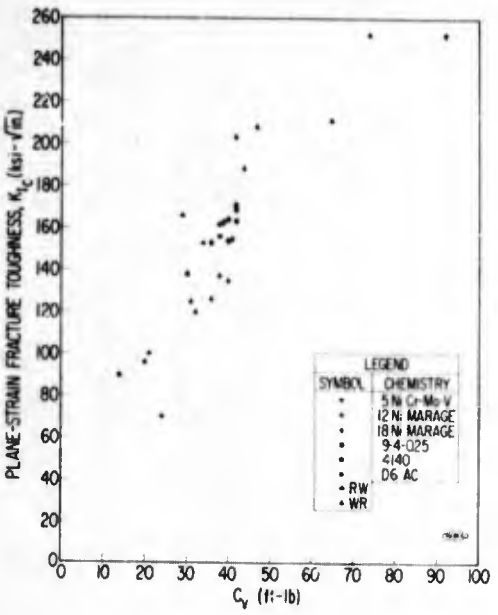

Fig. 12 - K_{Ic} versus Charpy-V energy for steel alloys at 32° F

quantitative estimations of these parameters from DT test results should be possible. Secondly, using the relationships provided by fracture mechanics between K_{Ic} and the critical flaw size and stress level for crack extension, the conditions for crack instability can be determined from the DT test energy.

ACKNOWLEDGMENTS

The authors are indebted to Dr. P. P. Puzak of NRL for his interest and helpful suggestions as well as the heat treatment and mechanical-property determination for the steels; to M. Cigledy, T. Snodgrass, and A. Kuntz for their aid in preparation and performance of the fracture-toughness tests; to R. W. Huber for his continuing interest in this effort; and to C. R. Forsht for the many feet of welds he prepared.

REFERENCES

1. Goode, R. J., and Huber, R. W., "Fracture Toughness Characteristics of Some Titanium Alloys for Deep-Diving Vehicles," J. Metals 17(No. 8):841-846 (1965).

2. Pellini, W.S., Goode, R.J., Puzak, P. P., Lange, E. A., and Huber, R. W., "Review of Concepts and Status of Procedures for Fracture-Safe Design of Complex Welded Structures Involving Metals of Low to Ultra-High Strength Levels," NRL Report 6300, June 1965

3. Sullivan, A. M., "New Specimen Design for Plane-Strain Fracture Toughness Tests," Materials Research and Standards 4(No. 1):20-24 (1964)

4. Gross, B., Srawley, J.E., and Brown, W. F., Jr., "Stress Intensity Factors for a Single-Edge-Notch Tension Specimen by Boundary Collocation of a Stress Function," NASA TN D-2396, Aug. 1964

5. Srawley, J.E., and Brown, W.F., Jr., "Fracture Toughness Testing," NASA TN D-2599, Jan. 1965.

6. Freed, C.N., and Krafft, J.M., "Effect of Side Grooving on Measurements of Plane-Strain Fracture Toughness," Journal of Materials 1(No. 4):770-790 (1966)

7. Krafft, J.M., "Fracture Toughness of Metals," Report of NRL Progress, pp. 4-16, Nov. 1963

8. Goode, R.J., et al., "Metallurgical Characteristics of High Strength Structural Materials (Seventh Quarterly Report)," NRL Report 6327, May 1965

9. Puzak, P.P., et al., "Metallurgical Characteristics of High Strength Structural Materials (Eighth Quarterly Report)," NRL Report 6364, Aug. 1965

10. Goode, R.J., et al., "Metallurgical Characteristics of High Strength Structural Materials (Tenth Quarterly Report)," NRL Report 6454, Apr. 1966

11. "The Slow Growth and Rapid Propagation of Cracks," ASTM Committee on Fracture Testing of High-Strength Metallic Materials, Materials Research and Standards 1(No. 5):389-393 (1961)

12. Boyle, R.W., Sullivan, A.M., and Krafft, J.M., "Determination of Plane-Strain Fracture Toughness with Sharply Notched Sheets," Welding J. Res. Suppl. 41: 428-S—432-S (1962)

Appendix A

K_{Ic} CALCULATION FOR FOUR-POINT-LOADED NOTCH-BEND SPECIMEN

The boundary collocation formula used to compute G_{Ic} for the four-point-loaded specimens is (5)

$$EG_{Ic} = \left(\frac{P}{B}\right)^2 \frac{L^2}{W^3} \left[34.7 \frac{a}{W} - 55.2 \left(\frac{a}{W}\right)^2 + 196 \left(\frac{a}{W}\right)^3\right], \tag{A1}$$

where

E = Young's modulus of elasticity

P = load at initial crack extension

B = specimen thickness

L = distance between a minor loading point and the nearest major loading point

W = specimen width

a = crack length (notch plus fatigue crack).

The strain-energy release rate at initial crack instability G_{Ic} is related to the critical value of the stress intensity factor K_{Ic} by

$$EG_{Ic} = (K_{Ic})^2. \tag{A2}$$

Appendix B

CALCULATION OF K_{Ic} WHEN SIDE GROOVES ARE EMPLOYED

The stress intensity factor for the SEN specimens was computed according to the experimental compliance calibration of Ref. 3, while the boundary collocation formula of Ref. 5 was used to calculate K_{Ic} for the NB specimens. The nominal stress intensity factor for both specimen types was determined, neglecting the presence of the side grooves; i.e., the thickness of the fracture plane was assumed to be equal to the thickness of the ungrooved specimen B. In terms of the strain-energy release rate, it is evident that the strain energy is working on only that thickness of plate which comprises the fracture plane B_n. Therefore, a thickness correction must be made by using

$$\mathcal{G}_{\text{nom}}\left(\frac{B}{B_n}\right) = \mathcal{G}_{Ic}, \tag{B1}$$

where $\mathcal{G}_{\text{nom}}$ is the nominal value of $\mathcal{G}$ calculated with the assumption that the side grooves were not present. The following equation expresses the correction in terms of the stress intensity factor:

$$K_{\text{nom}}\left(\frac{B}{B_n}\right)^{1/2} = K_{Ic}. \tag{B2}$$

For reasons described in Ref. 6 the thickness correction mentioned above is more complicated; the exponent is actually greater than 1/2 but less than 1. However, as it would be impractical to determine the specific exponent for each alloy, the exponent 1/2 was used throughout this report to compute K_{Ic}. By employing shallow side grooves, the error is kept small and will tend to cause the stress intensity factor to be slightly conservative.

Appendix C

COMPUTATION OF THE NOMINAL STRESS AT THE CRACK TIP

To obtain some knowledge as to whether the recorded crack instability occurred above or below the yield point, the nominal stress at the crack tip was calculated for each specimen. For the SEN specimen with the loading-pin centers on the specimen axis, the formula for calculating the nominal stress, σ_{nom}, is

$$\sigma_{nom} = \frac{P}{B(W-a)}\left(1 + \frac{3a}{W-a}\right) \tag{C1}$$

where

W = specimen width

B = specimen thickness

a = crack length (notch plus fatigue crack)

P = load at instability.

The nominal stress at the crack tip for the NB bars is found using the beam formula

$$\sigma_{nom} = \frac{Mc}{I}, \tag{C2}$$

where

M = moment (in four-point bending the length of the moment arm is the distance between a minor loading point and the nearest major loading point.)

c = distance between the neutral axis and the crack tip

I = moment of inertia.

On computing the nominal stress, it was compared with the yield stress, and the average ratio for each alloy and heat treatment is presented in Tables 3 and 5.

Appendix D

FRACTURE APPEARANCE

The method to calculate the proportion of the fracture surface which was occupied by shear lips is presented below. This method was applied to both the SEN and DT test specimens after fracture.

The distance between the fatigue crack or embrittled weld and the unnotched edge of the specimen was determined. At the midway point, measurement f (made across the specimen thickness B) was taken of the central flat fracture which existed between the shear lips. The percentage of fracture surface which was composed of shear lip at this point was determined by

$$\frac{(B - f)}{B} \cdot 100 = \text{percent shear lip.} \qquad \text{(D1)}$$

Security Classification

DOCUMENT CONTROL DATA - R & D

(Security classification of title, body of abstract and indexing annotation must be entered when the overall report is classified)

1. ORIGINATING ACTIVITY *(Corporate author)*
Naval Research Laboratory
Washington, D.C. 20390

2a. REPORT SECURITY CLASSIFICATION
Unclassified

2b. GROUP

3. REPORT TITLE
CORRELATION OF TWO FRACTURE TOUGHNESS TESTS FOR TITANIUM AND FERROUS ALLOYS

4. DESCRIPTIVE NOTES *(Type of report and inclusive dates)*
Interim report; work is continuing

5. AUTHOR(S) *(First name, middle initial, last name)*
C. N. Freed and R. G. Goode

6. REPORT DATE
January 16, 1969

7a. TOTAL NO. OF PAGES
28

7b. NO. OF REFS
12

8a. CONTRACT OR GRANT NO.
NRL Problem F01-07

b. PROJECT NO.
S-4607-11894

c.

d.

9a. ORIGINATOR'S REPORT NUMBER(S)
NRL Report 6740

9b. OTHER REPORT NO(S) *(Any other numbers that may be assigned this report)*

10. DISTRIBUTION STATEMENT
This document has been approved for public release and sale; its distribution is unlimited.

11. SUPPLEMENTARY NOTES

12. SPONSORING MILITARY ACTIVITY
Department of the Navy (Naval Ship Systems Command), Washington, D.C. 20360

13. ABSTRACT

High-strength ferrous and titanium alloys are of interest for use in complex structures, such as deep-diving vehicles and aircraft. A knowledge of the notch fracture toughness of these alloys is necessary to preclude catastrophic failure; however, experience indicates that no single test method itself can provide reliable fracture-toughness information across the whole toughness spectrum of these high-strength alloys.

A previously established relationship between the dynamic tear (DT) test (formally designated as the drop-weight tear test, DWTT) energy and the explosion tear test performance provides reliable fracture-toughness information of those alloys characterized by a toughness level requiring plastic deformation to propagate fracture. This analysis has not been extended to the ultrahigh-strength alloys in which fracture can propagate catastrophically at elastic stress levels. For these alloys, the analytical methods of linear elastic fracture mechanics provide the required elastic stress level and flaw-size relationship for fracture. This report deals with a "marriage" of the two approaches—the engineering and the analytical—by correlative techniques.

A direct correlation has been found to exist between the DT test energy for fracture and the critical stress intensity factor K_{Ic} for titanium alloys and steels. The relationship may also be

— Continues

DD FORM 1 NOV 68 1473 (PAGE 1)
S/N 0101-807-6801

Security Classification

14 KEY WORDS	LINK A		LINK B		LINK C	
	ROLE	WT	ROLE	WT	ROLE	WT
Fracture toughness						
High-strength steels						
Titanium alloys						
Dynamic tear test						
Linear-elastic fracture mechanics						
Elastic-strain energy						

expressed in terms of β_{Ic} - DT test energy or G_{Ic} - DT test energy. A correspondence was further established between β_{Ic} and fracture appearance as determined by the percentage of shear lip on the single-edge notch specimen. The Charpy V-notch test proved to be relatively insensitive to changes in fracture toughness of titanium alloys, and the results could not be correlated with K_{Ic}; however, such a relationship was established between these tests for steels.

The implication of this study is that reasonable estimates of plane-strain fracture toughness should be possible from results obtained from reliable engineering methods for measuring fracture toughness.